Int. J. Therm. Sci. (2000) 39, 18–29

S1290-0729(00)00200-2/FLA

Flow drag and heat transfer reduction of flowing water containing fibrous material in a straight pipe

Hideo Inaba *, Naoto Haruki, Akihiko Horibe

Department of Mechanical Engineering, Okayama University, 3-1-1 Tsushima-naka, Okayama, Japan, 700-8530

(Received 8 March 1999, accepted 7 August 1999)

Abstract — It has been well known that some kinds of surfactants are useful to reduce flow drag in a turbulent pipe flow by Toms effect. However, it is expensive to make these surfactants harmless to the environment. On the other hand, the fibrous material such as pulp fibers and cellulose are harmless additives to the environment. This paper deals with the drag reduction and heat transfer characteristics of the water suspension flow mixed with fine fibers in a circular straight pipe. Measurements of velocity and temperature profiles in a circular pipe were made in order to examine the flow drag and heat transfer characteristics of the turbulent and laminar flow. The nondimensional correlation equations of pipe flow resistance and heat transfer were derived in terms of various nondimensional parameters. © 2000 Éditions scientifiques et médicales Elsevier SAS

flow drag reduction / convection heat transfer / fibrous material / Toms effect / fiber suspension flow

Nomenclature

A	heat transfer area, also see equation (17)	m^2
a	plug radius ratio defined in equation (13)	m
C_p	mass density of pulp fiber	%
Cp	specific heat	$kJ{\cdot}kg^{-1}{\cdot}K^{-1}$
d_i	pipe inside diameter	m
d_o	pipe external diameter	m
d_p	pulp fiber diameter	m
h_c	convective heat transfer coefficient	$W{\cdot}m^{-2}{\cdot}K^{-1}$
k	thermal conductivity	$W{\cdot}m^{-1}{\cdot}K^{-1}$
L	average length	m
l	length	m
N	number	
Nu	Nusselt number	
ΔP	pressure drop	Pa
Pr	Prandtl number	
Q	heat transfer rate	W
R	pipe radius	m
r	radius	m
Re	Reynolds number	
S	standard deviation	
T	temperature	K
ΔT	temperature difference between the wall temperature of test section and bulk temperature of flowing water in a pipe	K
u	local velocity	$m{\cdot}s^{-1}$
u^+	nondimensional velocity	
U_m	the average velocity of a flowing fluid in a pipe	$m{\cdot}s^{-1}$
v^*	friction velocity	$m{\cdot}s^{-1}$
y	distance from a pipe wall	m
y^+	nondimensional length	

Greek Symbols

α	$(a^4 - 4a + 3)/(12a)$	
γ	shear rate	s^{-1}
δ	plug length from the wall	m
δ^+	nondimensional plug length from the wall	
η	viscosity	Pa·s
η_a	apparent viscosity of pulp fiber suspension	Pa·s
η_b	plastic viscosity	Pa·s
η_{spT}	viscosity ratio	
κ	Kármán number	
λ	coefficient of pipe friction	
ν	kinematic viscosity	$m^2{\cdot}s^{-1}$
ρ	density	$kg{\cdot}m^{-3}$
τ	shear stress	Pa
τ_y	yield stress	Pa

* Correspondence and reprints.
inaba@mech.okayama-u.ac.jp

τ_w wall shear stress . . . . . Pa

Subscripts

H heater
i, in entrance of the test section
m mean
p pulp fiber
w water or pipe wall
1 long pulp fiber
2 short pulp fiber

1. INTRODUCTION

Recently, the flow drag reduction effect achieved adding a turbulent control additive to the heat transport medium has attracted the attention of some researchers who have developed the effective thermal energy transport system in the pipe. In particular, it is well known that the flow resistance in a pipe for water solutions decreases remarkably by adding a small amount of surfactant (rodlike micells) or some kinds of polymers. This phenomenon is called the Toms effect, and many researches have actively investigated this effect. For example, Tomita [1, 2] has investigated the flow resistance and velocity distribution of the polyethylene oxide water solution, and Usui et al. [3] have also researched the heat transport system using the cationic surfactant (cetyltrimethyl ammonium chloride and oleyl-di-(2-hydroxyethyl)-methyl ammonium chloride) solution as a flow drag reduction additive. Furthermore, Park et al. [4] have examined the turbulent structure of the water solution with cetyltrimethyl ammonium chloride, and they have elucidated the dispersion effect of the turbulence energy of the surfactant solution by means of the velocity distribution measurement in detail. Fossa et al. [5] experimented on the flow resistance and heat transfer of the polymer solution. The authors have also reported previously the measurement result of the flow velocity distribution, the flow resistance and heat transfer characteristics of the water solution with the cationic surfactant (cetyltrimethyl ammonium bromide [6], and dodecyltrimethyl ammonium chloride [7]) and the polymer (polyethylene glycol [6]), and have also expressed by the nondimensional correlative equations. The obtained results showed that it was possible to reduce the pumping power, to downsize the transport system, to reduce the cost of the transport device, and to decrease the heat loss to the environment by using the surfactant water solution as a thermal energy transport medium.

However, some problems have been pointed out to use the surfactant solution as a thermal energy transport medium. Especially, the environmental pollution by discarding the used surfactant solution has become a serious problem. To solve this problem, Usui et al. [3] proposed the adsorption of the surfactant by means of activated carbon. Fundamentally, it is required that new additives having the same flow drag reduction effect as the surfactant solution and also a little environmental load are used.

The fiber, asbestos and solid particles have been reported as a flow drag reduction additive instead of surfactants and polymers used in the previous researches. For example, the usage of them has been reported by Katou et al. [8], Daily et al. [9] and Watanabe et al. [10]. Katou et al. [8] and Daily et al. [9] have mentioned only flow resistance of the fiber suspension, while Watanabe et al. [10] have reported the drag reduction phenomenon in water/fine solid particle suspensions. However, there were no experimental data on the heat transfer of the fiber suspension. However, there have been few reports, which examined the mechanism of the flow resistance and heat transfer characteristics of those suspension substances in the flowing water in detail.

In this present paper, the pulp fibers were selected as the most suitable additive having a little environmental impact and the flow drag reduction effect in the water suspension flow instead of the surfactant additive. The flow resistance and heat transfer coefficient of the pulp fiber water suspension as a cold heat transport medium has been measured in the present study. Furthermore, the mechanism of flow resistance and heat transfer characteristics has been examined by the measurement of the temperature and velocity distribution in a pipe. Finally, the fundamental information of the thermal energy transport system by using the fiber suspension for a little environmental impact has been provided in the present study.

2. FLOW DRAG REDUCTION ADDITIVE

The pulp fiber material as a new type of flow drag reduction additive was selected instead of the polymer or surfactant in the present study. The pulp fiber can be easily resolved in the nature since the pulp fiber consists of the vegetable fiber that forms paper. Therefore, the pulp fiber does not have a harmful effect on the environment, and it is promising material as a flow drag reduction additive. The main ingredient of the pulp fiber is the cellulose which is a kind of polysaccharide, and it is difficult to dissolve in water. Therefore, the liquid containing the pulp fibers as a dispersion phase is treated as suspension.

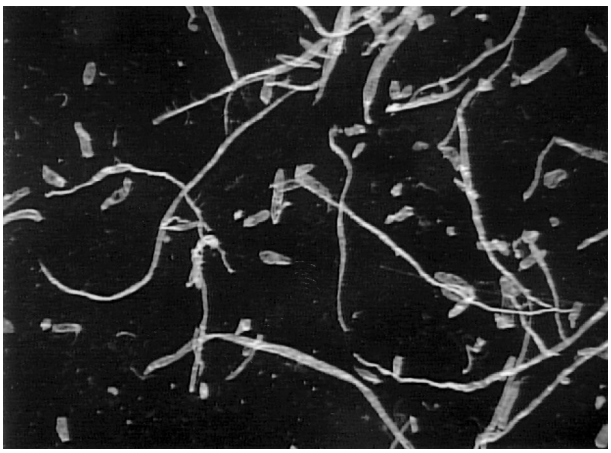

Figure 1. Photograph of the pulp fiber suspension in water.

The microscope video picture of the pulp fibers dispersing in water is shown in *figure 1*. The measuring method for length distribution of the pulp fibers was as follows. After the video pictures of them were taken at a magnification of 80, the number and length of them were estimated from the obtained video pictures. The video pictures of pulp fibers showed the pulp fiber diameter d_p to range between 6.45 μm and 29.0 μm. On the other hand, the data for the pulp fiber length could be divided into two groups. One was a long pulp fiber group in which fiber length is about 50 times longer than the pulp fiber diameter, and the other is a short pulp fiber group with a length of about 1–2 times the pulp fiber diameter. The reason why two groups of pulp fiber length were formed is because the pulp fibers were separated with a mixer (revolution diameter 12 mm, number of revolutions 8 000−24 000 rpm) which was used for mixing and dispersing the pulp fibers in water.

Figures 2 and *3* show the frequency distributions of the pulp fiber length for each pulp fiber group. From these results, it was found that the long pulp fiber group has the standard deviation of $S_{p1} = 0.347$ mm and average length of $L_{pm1} = 0.796$ mm, and the short pulp fiber group has the standard deviation of $S_{p2} = 0.0272$ mm and average length of $L_{pm2} = 0.0670$ mm. The volume ratio of the long fiber group to the short one was calculated to be 89.9 to 9.58 from the numbers of the long pulp fiber (113 pieces) and the short pulp fiber (148 pieces). It was clarified that the degradation of pulp fibers did not occur since the obtained volume ratio of fibers remained constant during the experiment.

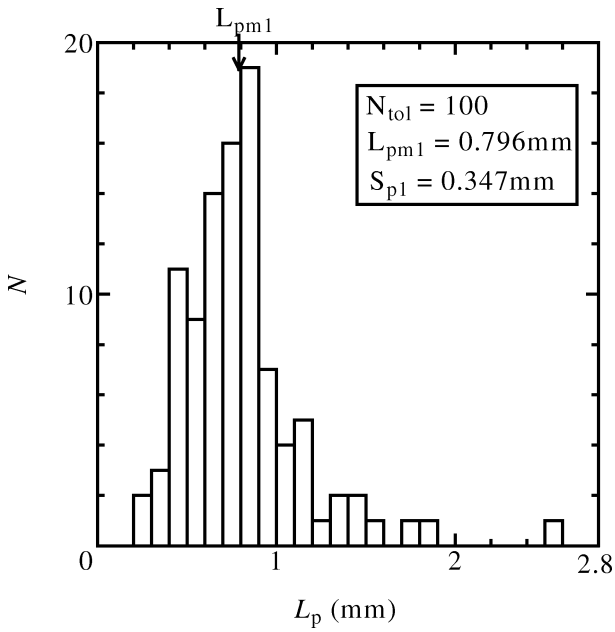

Figure 2. The long pulp fiber length distribution.

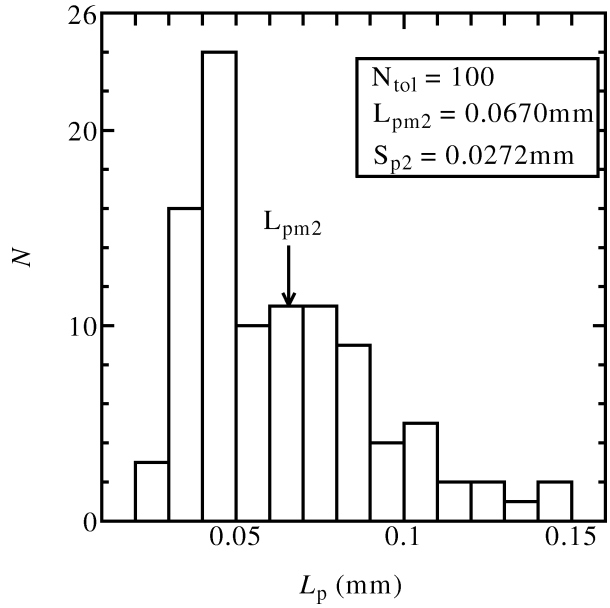

Figure 3. The short pulp fiber length distribution.

3. EXPERIMENTAL APPARATUS AND METHOD

The schematic diagram of the experimental apparatus for flow drag reduction and heat transfer measurement is presented in *figure 4*. As shown in *figure 4*, the exper-

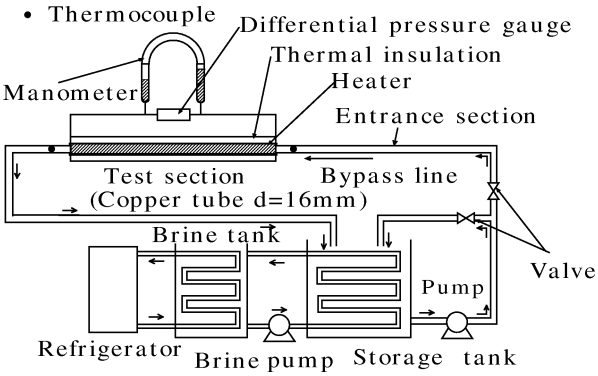

Figure 4. Schematic diagram of the experimental apparatus.

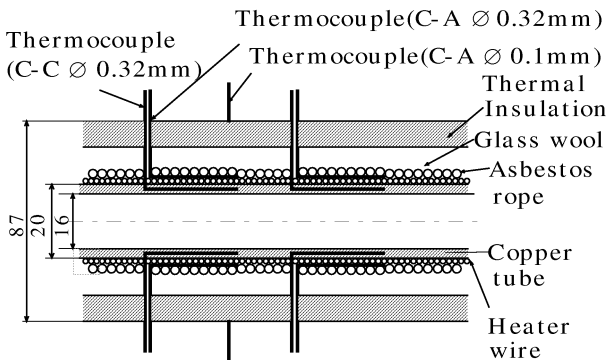

Figure 5. Schematic diagram of the heat transfer test section.

imental apparatus consisted of the pump, water storage tank, flow resistance and heat transfer measurement test section and pipelines. Furthermore, the temperature control device (the refrigerator, brine tank and brine pump) was installed into the water storage tank. Thus, it was possible to control the test fluid at desired temperature. Also some test pipes with various inside diameters and lengths were used to measure flow resistance and heat transfer. The velocity distribution of the fluid in the test pipes was measured with laser Doppler velocimeter. The temperature distribution of the fluid at the exit of the test section was measured with a thermocouple mounted on a traversing device.

A smooth circle pipe made of vinyl chloride, of inside diameter $d_\mathrm{i} = 16$ mm and length $l = 2.0$ m, was used for the flow resistance measurement in the test section. The present pipe was equipped with the entrance section having the enough length for fully developed hydrodynamic flow of the test fluid. In order to measure the friction coefficient λ of the test section, the water manometer (the minimum scale for the measurement 0.1 mm) and the difference pressure gauge (measurement accuracy $\pm 0.5\,\%$) were connected to the pressure tap (hole diameter 2.5 mm) mounted at the entrance and exit of the test section. The pipe friction coefficient was calculated by the following equation from the pressure drop (ΔP) measured in the test section:

$$\Delta P = \lambda \frac{l}{d_\mathrm{i}} \frac{1}{2} \rho U_\mathrm{m}^2 \tag{1}$$

While the tests to measure the flow resistance, the temperature of the pulp fiber water suspension was kept at 11–16 °C in the entrance of the test section in each test. The flow resistance was obtained by measuring the pressure drop of the test section ΔP and the mean velocity of test fluid U_m in the test section.

Figure 5 shows the details of the test section for heat transfer measurement. The heat transfer test section was incorporated into the experimental apparatus as shown in *figure 4*. The heat transfer test section consisted of a copper pipe (length of $l = 2$ m, outside diameter of $d_\mathrm{o} = 20$ mm, inside diameter of $d_\mathrm{i} = 16$ mm) and electric wire heaters insulated with glass fiber and wound evenly on the copper pipe outside. Each electric heater was divided into 12 sections. That is, the length of upstream side of the test section (5 section) was 120 mm and the length of the downstream side of it (7 section) was 200 mm. By adjusting the heater output for each section, the pipe wall temperature of the heat transfer test section could be controlled to the desired constant temperature. Therefore, the boundary condition of the heating surface corresponded to a constant wall temperature condition. The heat loss from the heaters to the environment through the thermal insulation material could be estimated within the maximum of 4.6 % of the electrical output.

During the measurement of heat transfer, the temperature of the pulp fiber water suspension at the entrance of the test section was kept at 12 ± 0.5 °C. The pipe wall temperature of each heat transfer test section was maintained at a constant temperature ($13–14 \pm 0.2$ °C). The heat transfer measurement was carried out by measuring the average heat transfer coefficient at various mean velocities of the test fluid in the pipe. The average heat transfer coefficient, h_c, was calculated by equation (2):

$$h_\mathrm{c} = \frac{1}{A \Delta T} \sum_{i=1}^{12} Q_\mathrm{i} \tag{2}$$

ΔT was the temperature difference between the wall temperature of the test section and bulk temperature of the test fluid. The bulk temperature of the pulp fiber water suspension has been calculated from the liner temperature distribution of the test fluid between inlet

and outlet of the test section due to small temperature difference between flow. In calculating equation (2), the physical properties of the test fluid were estimated at the average temperature between inlet and outlet temperature of the fluid.

The uncertainty of the obtained data on temperature was ±0.1 K, which was estimated by the thermocouple calibration and the temperature correction from the standard thermometer readings. The uncertainty of the pressure loss was estimated within $\pm 1.0 \cdot 10^{-4}$ Pa. The accuracy of the obtained heat flux measurement depended primarily on the heat loss from the heater to the environment and the error for the temperature measurement as a result. The uncertainly of the obtained heat flux was estimated within ± 0.8 W·m^{-2}. The error of the flow rate measurement depended mainly on the measuring accuracy of the mass flow rate, the time interval and the temperature, consequently, the uncertainty of the flow rate was estimated within ± 0.001 kg·s^{-1}. The corresponding uncertainty for the pipe friction coefficient λ, and Reynolds number was ±2.0 %, while the corresponding uncertainly for heat transfer coefficient h and Reynolds number was ±3.5 %.

Figure 6 shows the schematic diagram of laser Doppler velocimeter for the velocity distribution measurements in the test section. The LDV probe was generated by means of the He–Ne laser (10 mW, the intersection angle of 11.33°, focal length of 285 mm). The LDV probe was mounted on the traversing device with the positioning accuracy of 0.01 mm. The circle pipe made of glass (outside diameter $d_o = 20$ mm, inside diameter $d_i = 16$ mm) was used as the test section for velocity distribution measurements. The pipe was set in a water storage tank with a plane glass window (thickness of 1.0 mm) in order to reduce the refraction of the laser beam at the surface of a glass pipe. The Pitot tube (pipe inside diameter of 1.5 mm) was used for the measurement of the velocity distribution of the test water suspension inside the pipe since the pulp fibers interrupted the laser beam.

Furthermore, the temperature distribution of the test water suspension in the pipe was measured by the T-type thermocouple set at the exit of the heat transfer test section. The used thermocouples were copper–constantan thermocouples (wire diameter of 0.1 mm). The thermocouples were calibrated by means of a standard thermometer, so the measurement accuracy of the thermocouple was estimated within ±0.05 K. The thermocouple was shielded in stainless steel, and was fixed on test section pipe by a compression fitting in order to prevent the vibration of the thermocouple due to the flow of the suspension. The position of the thermocouple was measured by means of a micrometer (minimum indication of 0.01 mm).

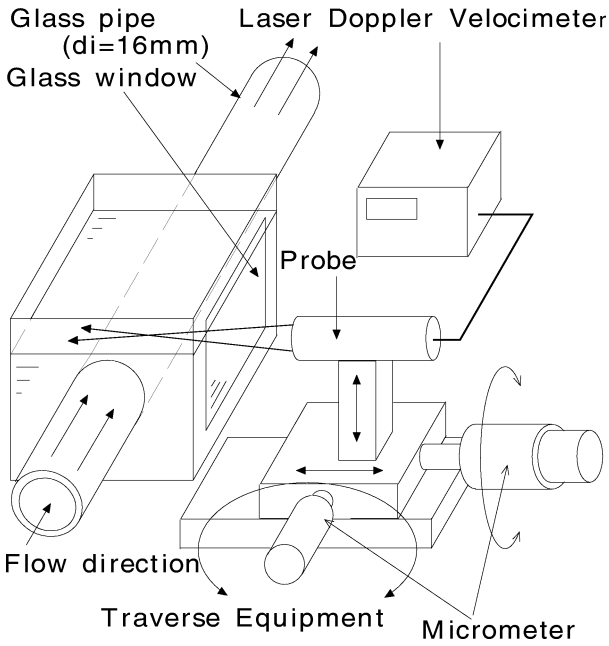

Figure 6. Schematic diagram of the LDV test section.

4. THE EXPERIMENTAL RESULTS OF THE VELOCITY DISTRIBUTION

4.1. The velocity distribution of the pulp fiber water suspension

According to Park et al. [4] and Usui et al. [3], the viscous sublayer thickness of flow drag reduction fluid (surfactant solution or polymer solution) showed the tendency to increase generally as compared with that of the Newtonian fluid. The authors measured the velocity distribution of surfactant solution in the pipe with laser Doppler velocimeter (LDV) in [6] and [7], and as a result, they came to get the same conclusion as Park. However, it was expected that the flow mechanism of the pulp fiber water suspension was different from that of the surfactant or polymer solution because the pulp fibers were dispersed in water without dissolving. Therefore, the measurement of the velocity distribution of the pulp fiber suspension has been made before the flow resistance and heat transfer measurements. At the same time, the flow pattern of the pulp fiber water suspension was observed, too.

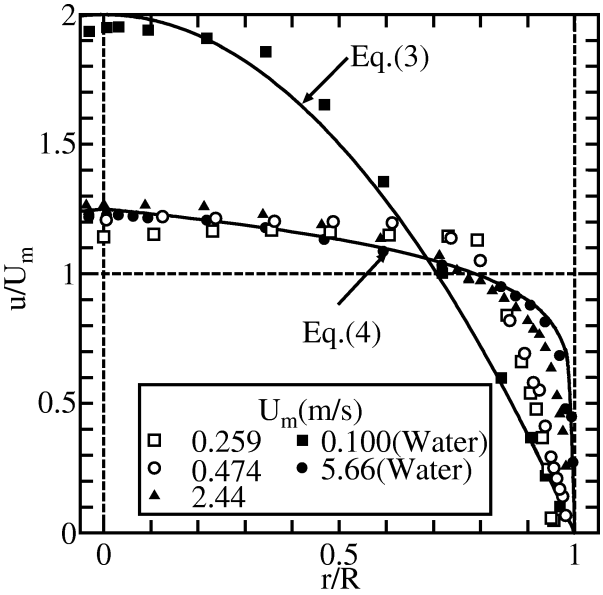

Figure 7. Relationship between u/U_m and r/R for $C_p = 0.65\,\%$.

First, the velocity distribution of flowing water in the pipe was measured in the present experimental apparatus. The results obtained for flowing water agreed with velocity distribution of the Newtonian fluid (equation (3) refers to the Poiseuille (laminar) flow, and equation (4) refers to the 1/7th power velocity distribution law of the turbulence flow) with a standard deviation of $\pm 2.0\,\%$. Consequently, the experimental accuracy of present experimental apparatus was judged to be sufficient to perform the present experiments.

$$\frac{u}{U_m} = 2\left\{1 - \left(\frac{r}{R}\right)^2\right\} \tag{3}$$

$$\frac{u}{U_m} = 1.224\left(1 - \frac{r}{R}\right)^{1/7} \tag{4}$$

Figure 7 shows the variation of velocity distribution of the pulp fiber water suspension (pulp fiber concentration $C_p = 0.65\,\%$) with nondimensional radius. In *figure 7*, the local velocity u was normalized by the bulk mean velocity U_m, and the radius r at a measuring position was normalized by the pipe radius R. However, the local velocity of $U_m = 2.44$ m/s in the range of $r/R = 0{-}0.8$ could not be measured with the LDV because the laser beam was disturbed by the pulp fibers. Therefore, the local velocity of the pulp fiber water suspension in that range was measured with a Pitot tube (the pipe inside diameter 1.5 mm). The Pitot tube was set at the same position in which the thermocouple for temperature distribution measurement was inserted. The pressure drop of the Pitot tube was measured with a manometer. The local velocity measured with the LDV at the point of $r/R = 0.8$ was in agreement with that with the Pitot tubes under the same flow rate condition. The average flow rate calculated by integrating the velocity profile obtained by the LDV and Pitot tube agreed with that obtained by water flowmeter with the standard deviation of $\pm 3.0\,\%$. Therefore, it was concluded that the appropriateness and the accuracy of the present measurement methods was sufficient for the velocity measurements.

From the later description of flow resistance experiment, it was confirmed that the pulp fiber water suspension in the turbulent flow region ($U_m = 2.44$ m·s^{-1}) in *figure 7* had the flow drag reduction effect. As shown in *figure 7*, the obtained velocity of the pulp fiber water suspension in the turbulent flow region in a pipe central part ($r/R = 0{-}0.75$) showed the tendency to exceed little that calculated by equation (4). On the other hand, the local velocity of the pulp fiber water suspension near the pipe wall ($r/R = 0.75{-}1$) was below that by equation (4). This tendency of velocity profile was similar to that of the surfactant solution that had the flow drag reduction effect in the previous report [6, 7].

The local velocity of the pulp fiber water suspension in the laminar flow ($U_m = 0.474$ and 0.259 m·s^{-1}) as shown in *figure 7* did not show the same tendency of Poiseuille flow. The local velocity of the pulp fiber water suspension in the laminar flow remained constant in the pipe central part ($r/R = 0{-}0.75$), and its tendency was similar to that of a plug flow. The obtained tendency resembled one observed by Bingham [11]. The rheology equation of Bingham fluid is defined by the following equation (5):

$$\tau_w = \tau_y + \eta_b \gamma \tag{5}$$

(τ_y: the yield stress, η_b: the plastic viscosity). The yield stress, τ_y, and the plastic viscosity, η_b, in equation (5) correspond to physical properties. In the pulp fiber suspension, the value of r_y/R $(= a)$ which kept at a constant velocity became 0.75 for various average velocities. Therefore, the yield stress τ_y $(= a\tau_w)$ of the pulp fiber water suspension was altered by the wall shearing stress (τ_w). The pulp fiber water suspension was different in its property from the Bingham fluid whose yield stress corresponded to physical property. The reason why the pulp fiber water suspension was not the Bingham fluid was because the pulp fibers were unevenly dispersed in the pipe by means of the local velocity distribution. In this paper, *figure 7* shows the typical local velocity distribution of the pulp fiber water suspension. If the pulp fiber concentration differs from

0.65 %, the range of constant local velocity in the laminar flow is similar to data in *figure 7*, while the local velocity distribution in the turbulent flow would be influenced by the pulp fiber concentration.

4.2. Nondimensional velocity distribution of the pulp fiber water suspension

Regarding the velocity profile of the pulp fiber water suspension normalized by the friction velocity and kinematic viscosity, Katou et al. [8] proposed the nondimensional velocity profile correlation equation for the fiber suspension by dividing the flow into two nondimensional distance regions, i.e. a viscous sublayer ($0 \le y^+ \le \delta^+$) and a logarithmic layer ($\delta^+ \le y^+ \le R$). δ^+ was defined by $\delta^+ = v^*\delta/\nu$, and y^+ was defined by $y^+ = v^* y/\nu$, which was normalized by the friction velocity v^* ($= (\tau_0/\rho)^{1/2}$). In the present study, it was examined whether the velocity profile equation by Katou et al. could be applied the obtained data or not.

According to Katou et al., the nondimensional velocity profile of the Newtonian fluid was proposed by equations (6) and (7) in case of using Newtonian nondimensional wall range thickness, δ^+, normalized by the friction velocity, v^*.

- Near-wall layer:

$$u^+ = F_1(y^+, \delta^+, \kappa) = y^+ - \delta^+\left(1 - \frac{1}{\kappa\delta^+}\right)\left\{\left(\frac{y^+}{\delta^+}\right)^4 - 0.6\left(\frac{y^+}{\delta^+}\right)^5\right\} \quad (6)$$

- Logarithmic layer:

$$u^+ = F_2(y^+, \delta^+, \kappa) = \frac{1}{\kappa}\ln y^+ + 0.60\,\delta^+ - \frac{\ln\delta^+ - 0.40}{\kappa} \quad (7)$$

For example, if equations (6) and (7) are applied for water, two unfixed numbers become $\delta^+ = 20$ and $1/\kappa = 2.5$.

If equations (6) and (7) are applied to the pulp fiber water suspension, the viscosity ratio of the pulp fiber suspension to water had to be $1 + \eta_{spT}$. The nondimensional turbulence velocity profiles of the pulp fiber water suspension could be defined in equations (8) and (9) by using nondimensional distance y_w^+ normalized by the viscosity of water and the viscosity ratio $1 + \eta_{spT}$.

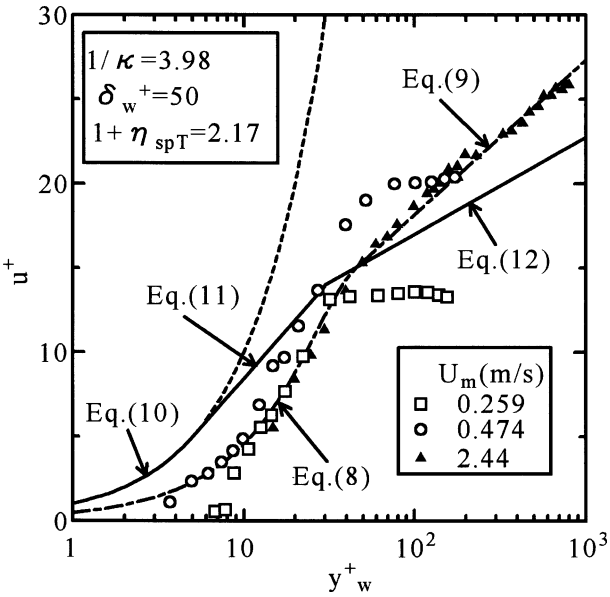

Figure 8. Relationship between u^+ and y_w^+.

- Wall range:

$$u^+ = F_1\left(\frac{y_w^+}{1+\eta_{spT}}, \frac{\delta_w^+}{1+\eta_{spT}}, \kappa\right) \quad (8)$$

- Logarithmic layer:

$$u^+ = F_2\left(\frac{y_w^+}{1+\eta_{spT}}, \frac{\delta_w^+}{1+\eta_{spT}}, \kappa\right) \quad (9)$$

Figure 8 shows the nondimensional velocity profile of the pulp fiber water suspension normalized by the viscosity of water and the friction velocity. Furthermore, equations (10)–(12) in *figure 8* are the universal velocity profile in the viscous sublayer, transition layer and turbulent region of the Newtonian fluid given by von Kármán.

- Viscous sublayer:

$$u^+ = y^+ \quad (10)$$

- Transition layer:

$$u^+ = 5.0\ln y^+ - 3.05 \quad (11)$$

- Turbulent region:

$$u^+ = 2.5\ln y^+ + 5.5 \quad (12)$$

As shown in *figure 8*, it was seen that the measured local velocities in the turbulent flow ($U_m = 2.44$ m·s^{-1}) and the laminar flow ($U_m = 0.474$ and 0.259 m·s^{-1})

near the pipe wall (small y_w^+) were below ones from equation (10). The obtained small velocities would be explained by the fact that the viscosity of water was used instead of the viscosity of the pulp fiber water suspension for nondimensionalization. This fact would mean that the apparent viscosity of the pulp fiber water suspension was greater than that of water. On the other hand, referring to the flow behavior in the pipe center region (large y_w^+), the local velocity in the laminar flow remained constant since the flow behavior was similar to the plug flow. It was found that the local velocity, u^+, showed the tendency to increase with increasing average velocity U_m. For the high velocity flow region, the gradient of u^+ to y_w^+ in the range of $y_w^+ \geq 50$ was reduced as compared with that near the pipe wall, but the value of u^+ showed the tendency to increase.

The curve indicated by the dash and dot line $(-\cdot-)$ in *figure 8* shows the calculation result of the nondimensional turbulence velocity profile in equations (8) and (9) in the case of the pulp fiber water suspension. On calculating equations (8) and (9), the viscosity ratio $1+\eta_{spT}$ of the pulp fiber water suspension had not yet been known, since the real viscosity of the pulp fiber water suspension could not be obtained in the present experiment. Therefore, the values of three undefined numbers (viscosity ratio $1+\eta_{spT}$, δ_w^+, κ) of the pulp fiber water suspension were estimated as follows.

First of all, the thickness of the near wall layer was determined as $\delta_w^+ = 50$ from the result of *figure 8* because the gradient of u^+ to y_w^+ in $U_m = 2.44\ \mathrm{m{\cdot}s^{-1}}$ changed at $y_w^+ = 50$. After that, the experimental correlation equation of u^+ with y_w^+ in the logarithmic layer ($\delta_w^+ \geq 50$) was obtained from the measurement data. Two undefined numbers ($1+\eta_{spT}$, κ) were estimated by comparing the obtained experimental correlation equation with equation (9). The obtained values of those undefined numbers were indicated in *figure 8*. Furthermore, the nondimensional velocity profile equation for near wall layer range of the pulp fiber water suspension could be calculated by substituting those undefined numbers to equation (8). The obtained results from equation (8) were in agreement with the experimental data with the standard deviation of $\pm 9.8\,\%$. In this way, the velocity profile of the pulp fiber water suspension could be predicted by the nondimensional turbulence velocity profile equations (8) and (9) proposed by Katou et al.

5. EXPERIMENTAL RESULTS OF FLOW RESISTANCE IN A PIPE

5.1. The viscosity of the pulp fiber water suspension

Regarding the nondimensional equation of flow resistance of the pulp fiber water suspension, the viscosity of the pulp fiber water suspension was necessary in order to calculate the Reynolds number that was usually used as a nondimensional parameter of mean flow velocity. However, as shown in *figure 7*, the velocity profile of the pulp fiber water suspension in the laminar flow was different from the common Poiseuille flow. That flow pattern was similar to the plug flow that had a constant velocity in the pipe center region. Therefore, it was understood that the flow behavior of the pulp fiber water suspension in the laminar flow was similar to that in the Bingham fluid flow. Because of this behavior of velocity profile, it was seen that the viscosity measurement of the pulp fiber water suspension with the capillary viscometer could not be adopted due to the size effect of the capillary pipe diameter. The viscosity measurement with a rotating viscometer could not be made owing to the uneven dispersion of the pulp fibers in the rotating water layer in the viscometer. For those reasons, viscosity η_a of the Bingham fluid proposed by Tomita [11] was used as the viscosity of the pulp fiber water suspension.

On the Bingham fluid, the pressure drop ΔP in the pipe (pipe length l) was defined in the following equation (13) by using the relation of the Bingham fluid rheology (equation (5)). By comparing the equation (13) with Hagen–Poiseuille equation of Newton fluid, the viscosity η_a of Bingham fluid was expressed in equation (14). The data of flow resistance (pressure drop ΔP) was nondimensionalized by the defined viscosity. The obtained data for pipe friction coefficient as nondimensional parameters agreed with that from equation (15) in the laminar flow.

$$\frac{\Delta P}{l} = \frac{8Q\{\eta_b/(4a\alpha)\}}{\pi R^4} \tag{13}$$

$$\eta_a = \frac{\eta_b}{4a\alpha} \tag{14}$$

Here, the parameter a corresponds to the radius ratio of the plug. The α is expressed as $\alpha = (a^4 - 4a + 3)/(12a)$.

As mentioned in the foregoing section, the pulp fiber water suspension could not be treated as a Bingham fluid because yield stress and plastic viscosity of pulp fiber water suspension cannot be regarded to be a physical property. In the present study, the pulp fiber water

TABLE I
The pulp fiber water suspension viscosity.

C_p (%)	0.15	0.30	0.52	0.55	0.60	0.70
T_p (°C)	12	12	12	12	15–18	12
η_a (mPa·s)	2.38	3.08	3.48	4.41	3.79	5.67

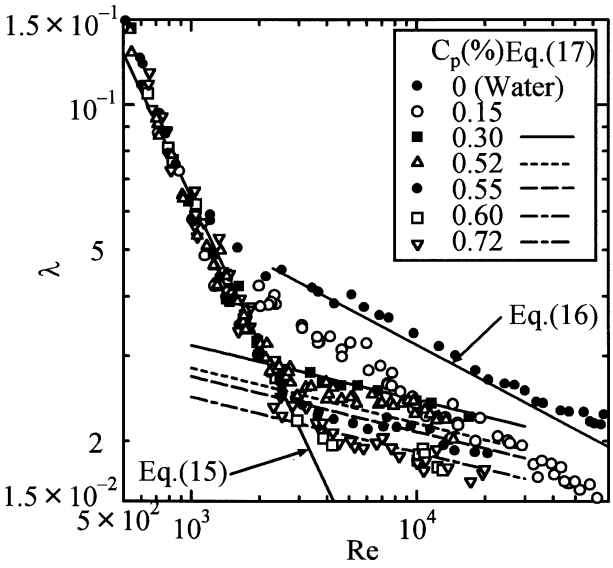

Figure 9. Relationship between λ and *Re*.

suspension was treated as a quasi-Bingham fluid. The calculated viscosity η_a of the pulp fiber water suspension for various concentrations is presented in *table I*. The data used for calculating viscosity η_a belonged only to the plug flow. Therefore, the a was equal to 0.75. In *table I*, the T_p refers to the pulp fiber water suspension temperature.

5.2. The nondimensional correlation of the pulp fiber suspension

Figure 9 presents the relationship between the pipe friction coefficient, λ, of the pulp fiber suspension in equation (1) and the Reynolds number, *Re*, defined using the viscosity in *table I*. In *figure 9*, equation (15) means the theory equation of the flow resistance in the laminar flow in a pipe, and equation (16) means the Blasius resistance formula for turbulent flow:

$$\lambda = \frac{64}{Re} = \frac{64}{U_m d_i/\nu} \tag{15}$$

$$\lambda = 0.3164 Re^{-0.25} = 0.3164(U_m d_i/\nu)^{-0.25} \tag{16}$$

From *figure 9*, it was seen that the pipe friction coefficient, λ, of the pulp fiber water suspension was consistent with equation (15) in the range of $Re \leq 2\,000$ for various pulp fiber concentrations C_p. On the other hand, in the case of $C_p = 0.15\,\%$, λ in the range of $Re \geq 2\,000$, increased at near $Re = 2\,000$, and then it was below by 15−20 % as compared with that from equation (16). However, the gradient of λ to *Re* for the pulp fiber water suspension was the same as that from equation (16). From the relationship between the pressure drop to every unit length ($\Delta P/l$) and the mean velocity (U_m) in the turbulent flow, it was found that $\Delta P/l$ of the pulp fiber water suspension agreed with the pressure drop gradient of the water from equation (16). Therefore, it was concluded that the flow drag reduction effect did not take place in the present flow region. The pressure drop characteristics of the pulp fiber water suspension showed the different tendency to that of Newtonian fluid since the turbulence structure of the pulp fiber water suspension differed from that of the Newtonian fluid.

On the other hand, the data of λ in the range of $C_p \geq 0.30\,\%$ showed the tendency to agree with those from the laminar flow equation (15) up to $Re = 3\,000$. And then as *Re* increased, the λ followed equation (15) and finaly it reduced and approached the value from equation (16). From those results, it was seen that the flow drag reduction effect at $C_p = 0.30\,\%$ took place, as a result, the λ of the pulp fiber water suspension in the turbulent flow was fairly lower than that of water. And it decreased with an increase in concentration, C_p. However, for $C_p \geq 0.60\,\%$, the value of λ was independent of C_p, since λ remained almost constant with increasing C_p in the range of $C_p \geq 0.60\,\%$.

In the range in which the pulp fiber water suspension had the flow drag reduction effect, the correlation equation (17) for the pipe friction coefficient λ was derived by the least-squares method. The maximum deviation of experimental data with equation (17) was 9.5 %. The calculation results from the equation (17) are presented in *figure 9*.

$$\lambda = A\,Re^{-0.114}$$
$$A = \begin{cases} 0.0702 - 0.203 C_p^5, & C_p \leq 0.609 \\ 0.0530, & C_p \geq 0.609 \end{cases} \tag{17}$$

Applicability range:

$$\left(\frac{64}{A}\right)^{1.13} \leq Re \leq \left\{\left(\frac{0.3164}{A}\right)\left(\frac{\eta_w}{\eta_p}\right)^{0.25}\right\}^{7.35}$$

Also, most of the thermal boundary layer in *figure 12* as shown in Section 6.2 existed in the ranges of I

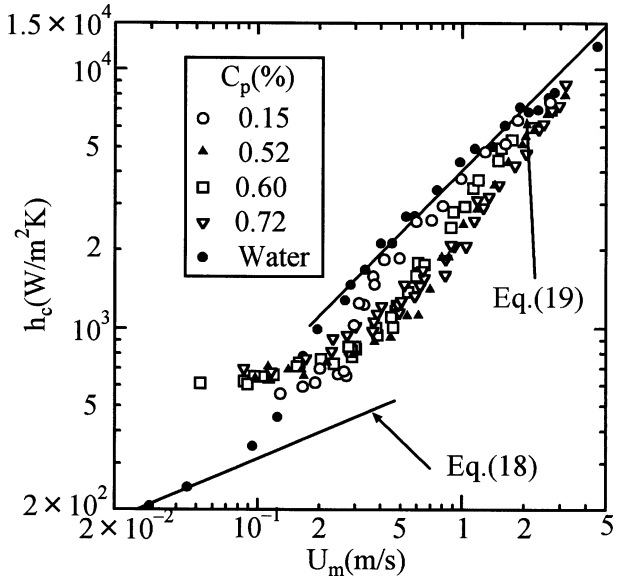

Figure 10. Relationship between h_c and U_m.

and II near the pipe wall. Therefore, it is concluded that the experimental correlation equation (17) could be applied in the range of pipe inside diameter $d_i \geq 16$ mm. However, referring to the smaller pipe diameter, it is necessary to investigate the pipe size effect since the shear stress from the pipe wall exerts an influence on the fluid flow in the center of pipe.

6. EXPERIMENTAL RESULTS OF HEAT TRANSFER IN A PIPE

6.1. Heat transfer characteristics of the pulp fiber water suspension

Figure 10 shows the relationship between the mean velocity, U_m, and the average heat transfer coefficient, h_c, of the pulp fiber water suspension under the uniform pipe wall temperature condition. The test section for the heat transfer measurement as shown in *figure 5* was used. In *figure 10*, two solid lines correspond to the relationship between the mean velocity, U_m, and the average heat transfer coefficient, h_c, of water calculated from equations (18) and (19), respectively. Equations (18) and (19) refer to the fully developed heat transfer coefficients in the laminar flow and the turbulent flow of water, respectively:

$$Nu = 1.86\left(Re\,Pr\frac{d_i}{l}\right)^{1/3}\left(\frac{\eta}{\eta_w}\right)^{0.14} \tag{18}$$

$$Nu = 0.027Re^{0.8}\,Pr^{1/3}\left(\frac{\eta}{\eta_w}\right)^{0.14} \tag{19}$$

In equations (18) and (19), the η corresponds to the viscosity in the bulk temperature of fluid and the η_w means the viscosity based on the pipe wall temperature. The measured results of water in this experimental apparatus agreed well with equations (18) and (19). From this fact, it was understood that the experimental accuracy of the experimental apparatus was sufficient in order to measure the heat transfer.

As shown in *figure 10*, the average heat transfer coefficient h_c of the pulp fiber water suspension was about two times larger than that from equation (18) in the low velocity flow range ($U_m \leq 0.4$ m·s^{-1}) for various pulp fiber concentrations C_p. It was supposed that the flow condition pertained to the laminar flow by judging from the pressure drop measurement results (*figure 9*). On the other hand, as the mean velocity U_m increased, the flow pattern be came turbulent, and as a result, the value of h_c in the range of $C_p \geq 0.52$ % was below that from the turbulent heat transfer equation (19). For higher velocity of U_m, the value of h_c approached to that from equation (19). It was elucidated that the pulp fiber water suspension had the heat transfer reduction effect in the turbulent flow. In case of $C_p = 0.15$ % in which the flow drag reduction effect in the turbulence flow could not be obtained in *figure 9*, h_c was greater than those of other concentrations and it became the same value from equation (19) in the range of $U_m \geq 0.6$ m·s^{-1}. Therefore, it was concluded that the heat transfer reduction effect could not take place.

Figure 11 shows the plots $Nu/Pr^{1/3}$ against Reynolds number *Re*. The *Nu* number and the *Pr* number were defined by equations (20) and (21), respectively:

$$Nu = \frac{\alpha d_i}{k_w} \tag{20}$$

$$Pr = \frac{\eta Cp_w}{k_w} \tag{21}$$

where thermal conductivity, k_w, and specific heat, Cp_w, were estimated by the physical properties of water, and the η was defined by the apparent viscosity of the pulp fiber water suspension.

As shown in *figure 11*, it was seen that $Nu/Pr^{1/3}$ of the pulp fiber water suspension in the range of $Re \leq 2\,000$ was greater than that from the laminar heat transfer equation (18) as shown in *figure 10*. While, the values of $Nu/Pr^{1/3}$ in the turbulent flow ($Re \geq 2\,000$) were a greater value than those from the turbulent heat transfer equation (19). From *figure 11*, it could be noticed that

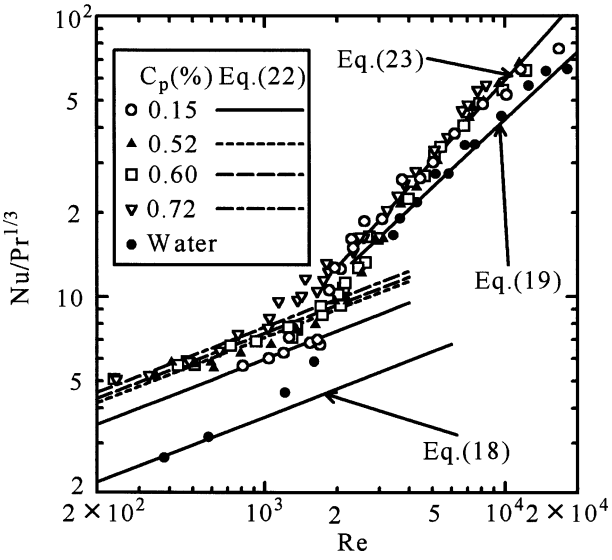

Figure 11. Relationship between $Nu/Pr^{1/3}$ and Re.

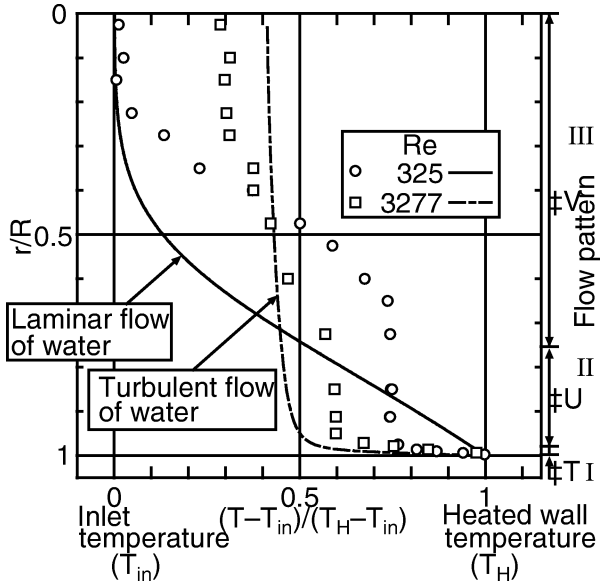

Figure 12. Relationship between T and r/R.

the value of $Nu/Pr^{1/3}$ is to a lesser extent dependent on pulp fiber concentration. In *figure 11*, the increasing tendency of $Nu/Pr^{1/3}$ more than that from equation (19) was brought by using the viscosity on the basis of the Bingham fluid for calculating *Re* number in the laminar flow. It is necessary to obtain the apparent viscosity of the pulp fiber water suspension.

6.2. Temperature distribution of the pulp fiber suspension in a pipe

As shown in *figures 10* and *11*, the heat transfer characteristics of the pulp fiber water suspension showed the special tendency that the heat transfer in the laminar flow increased as compared with that of only water. In order to find the reason of the present special heat transfer characteristics, the temperature profile of the pulp fiber water suspension was measured with the local temperature measurement thermocouple attached to the exit of the test section. In the temperature profile measurement of the pulp fiber suspension, the inlet temperature of the pulp fiber water suspension was $19.9 \pm 0.1\,^{\circ}\mathrm{C}$, the pulp fiber concentration C_p was 0.63 %, and the heat wall temperature was kept at $22.0 \pm 0.1\,^{\circ}\mathrm{C}$ (constant wall temperature condition). *Figure 12* shows the measured results of the temperature profile of water and pulp fiber water suspension. In comparing the measured results of water with the numerical calculation results, both results agreed with each other with the maximum deviation of 0.1 K.

As shown in *figure 12*, it was seen that the temperature of the pulp fiber water suspension in the laminar flow ($Re = 325$) dropped suddenly as compared with that of water near the pipe wall (the range of I, as shown on the right side of *figure 12*). However, the local temperature in the range from the pipe wall to $r/R = 0.75$ (range II) remained constant. On the other hand, the temperature profile in the pipe central region (the plug flow range in *figure 8*, range III, $r/R = 0{-}0.75$) was similar to the parabolic temperature one. In the range of I and II, the pulp fibers (or the lump of fibers) were deformed and moved with circulation by the shearing. This circulation of the pulp fibers (or the lump of fibers) in the water suspension induced the secondary flow. And increase of the temperature gradient of the pulp fiber water suspension near the wall would be related to this secondary flow, and the laminar heat transfer of the pulp fiber water suspension was increased by the secondary flow. Furthermore, in the range of III, the pulp fibers cohered as a lump of fibers were flowing in the center of pipe. However, in the range of I and II, it was observed that separation and cohesion of the lump of fibers was repeated by the secondary flow. The pulp fibers could be pumped without suffering any degradation or agglomeration, and they were randomly and uniformly distributed in the test section without very low flow velocity beyond the range of the present experimental conditions.

On the other hand, referring to the temperature profile of the pulp fiber water suspension in the turbulent region

of $Re = 3\,277$, it is seen that the difference of the local temperature between the pipe center and the pipe wall decreased, and the temperature profile was similar to that of only water flow in the turbulence flow. However, the temperature gradient near the pipe wall of the pulp fiber water suspension became smaller than that of turbulent flow of water. From the obtained results, it was confirmed that the heat transfer of the pulp fiber water suspension was reduced in the turbulent flow region.

From the data for the heat transfer of the pulp fiber water suspension, the experimental correlation equations (22) and (23) of $Nu/Pr^{1/3}$ with Re number were derived with the maximum deviation of $\pm 9.5\,\%$ by the least squares method. The calculation results of these equations are shown in *figure 11*.

- Laminar:

$$\frac{Nu}{Pr^{1/3}} = (0.550 + 0.315 C_{\mathrm{p}}) Re^{1/3} \qquad (22)$$

- Turbulent:

$$\frac{Nu}{Pr^{1/3}} = 9.21 \cdot 10^{-3} Re^{0.952} \qquad (23)$$

7. CONCLUSION

With regard to the heat energy transport system using the flow drag reduction effect, the velocity and temperature distribution, the flow resistance and heat transfer characteristics of water suspension with the pulp fiber were measured in the present study. The following conclusions were obtained.

(1) From the experimental results of the velocity distribution of the pulp fiber water suspension, the flow tendency similar to a plug flow was obtained in the laminar flow. It was clarified that the flow condition of the pulp fiber water suspension differed from that of the surfactant solution. Furthermore, the previous estimation method for the nondimensional velocity distribution equation could be applied to the pulp fiber water suspension.

(2) From the flow resistance data of the pulp fiber water suspension, the flow drag reduction effect was observed. By using the viscosity of the pulp fiber water suspension obtained by supposing the laminar flow as a Bingham fluid, the nondimensional correlation equation for the flow resistance was derived by means of some parameters.

(3) The enhancement effect of heat transfer in the laminar flow and the heat transfer reduction effect in the turbulent flow were elucidated by the heat transfer measurements for the pulp fiber water suspension. It was found that the phenomenon of heat transfer enhancement in laminar flow was dependent on the secondary flow by the circulation of the fibers or the lump of the fibers.

These conclusions are effective against the same type of the pulp fibers used in the present study. However the whole tendency of the flow drag and heat transfer reduction effect are the same as those in the present study.

REFERENCES

[1] Tomita Y., Trans. Jpn. Soc. Mech. Eng. 35-279 (1969) 2243–2250.

[2] Tomita Y., Trans. Jpn. Soc. Mech. Eng. 35-279 (1969) 2251–2258.

[3] Usui H., Saeki T., Takagi T., Tokuhara K., Evaluation of pumping power consumption in direct heating and cooling system with drag reducing cationic surfactants, and discussions on the practical application of surfactant drag reduction, Kagaku Kogaku Ronbunshu 21(2) (1995) 248–256.

[4] Park S.R., Yoon H.K., Kawaguchi Y., Experimental study of turbulence characteristics in drag reducing channel flows with 2D-LDV, in: Proceedings of the 3rd KSME-JSME Thermal Engineering Conference, Kyongju, Korea, 1996, pp. III-221–226.

[5] Fossa M., Tagliafico L.A., Experimental heat transfer of drag-reducing polymer solutions in enhanced surface heat exchange, Exp. Thermal Fluid Sci. 10 (1995) 221–228.

[6] Inaba H., Ozaki K., Haruki N., Asano H., Flow resistance and heat transfer characteristics of water solution flow with surfactant in circular tubes, Trans. Jpn. Soc. Mech. Eng. 61-589 B (1995) 3304–3310.

[7] Inaba H., Haruki N., Flow resistance and heat transfer characteristics of cold water pipe flow with surfactant for cold heat energy transport, Trans. Jpn. Soc. Mech. Eng. 63-589 B (1997) 1336–1343.

[8] Kato H., Mizunuma H., Trans. Jpn. Soc. Mech. Eng. 48-430 B (1982) 1066–1074

[9] Daily J.W., Bugliarello G., A particular non-Newtonian flow, Ind. Eng. Chem. 51-7 (1959) 887–888.

[10] Watanabe K., Ohira H., Kato H., Drag reduction phenomenon in water/fine solid particle suspension, Trans. Jpn. Soc. Mech. Eng. 58-548 B (1992) 1056–1062.

[11] Tomita Y., Rheology, Korona Inc., 1975.